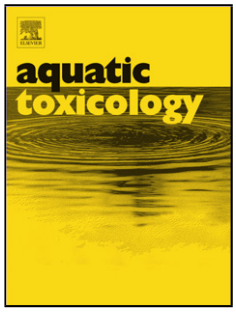

Title: Co-exposure of the organic nanomaterial fullerene C_{60} with benzo[a]pyrene in *Danio rerio* (zebrafish) hepatocytes: Evidence of toxicological interactions

Author: Ferreira Josencler L. Ribas Lonné María Noelia A. França Thiago R. Maximilla Naiana Thiago H. Lugokenski Patrícia G. Costa Fillmann Gilberto Félix A. Antunes Soares Fernando R. de la Torre Monserrat José María

PII: S0166-445X(13)00348-2
DOI: http://dx.doi.org/doi:10.1016/j.aquatox.2013.12.007
Reference: AQTOX 3702

To appear in: *Aquatic Toxicology*

Received date: 31-5-2013
Revised date: 4-12-2013
Accepted date: 7-12-2013

Please cite this article as: Ferreira, Ribas, J.L., Noelia, M., Thiago, A.F., Naiana, R.M., Lugokenski, T.H., Costa, P.G., Gilberto, F., Torre, F.A.A.S., </sup>,Fernando R. de la, María, M.J.,Co-exposure of the organic nanomaterial fullerene C_{60} with benzo[a]pyrene in *Danio rerio* (zebrafish) hepatocytes: Evidence of toxicological interactions, *Aquatic Toxicology* (2013), http://dx.doi.org/10.1016/j.aquatox.2013.12.007

Co-exposure of the organic nanomaterial fullerene C_{60} with benzo[a]pyrene in *Danio rerio* (zebrafish) hepatocytes: Evidence of toxicological interactions

Ferreira, Josencler L. Ribas[1,2,4*], Lonné, María Noelia[5], França, Thiago A.[1], Maximilla, Naiana R.[1], Lugokenski, Thiago H.[6], Costa, Patrícia G.[3], Fillmann, Gilberto[3], Antunes Soares, Félix A.[6], de la Torre, Fernando R.[7], Monserrat, José María [1,2,4,8]

[1] Universidade Federal do Rio Grande – FURG, Instituto de Ciências Biológicas (ICB), Campus Carreiros, Av. Itália km 8 s/n (96200-970), Rio Grande, RS, Brasil.

[2] Programa de Pós Graduação em Ciências Fisiológicas – Fisiologia Animal Comparada, Instituto de Ciências Biológicas (ICB), FURG.

[3] Laboratório de Microcontaminantes Orgânicos e Ecotoxicologia Aquática (CONECO), Instituto de Oceanografia (IO), FURG.

[4] Rede de Nanotoxicologia (MCTI/CNPq), Nanotoxicologia ocupacional e ambiental: subsídios científicos para estabelecer marcos regulatórios e avaliação de riscos, Rio Grande, RS, Brasil.

[5] Universidad de Buenos Aires, Facultad de Ciencias Exactas y Naturales, Buenos Aires, Argentina.

[6] Universidade Federal de Santa Maria (UFSM), Departamento de Química, Santa Maria, RS, Brasil.

[7] Universidad Nacional de Luján, Departamento de Ciencias Básicas, Buenos Aires, Argentina.

[8] Instituto Nacional de Ciência e Tecnologia de Nanomateriais de Carbono (CNPq)

*Corresponding author

Phone: +55 53 32935175

E-mail address: josenclerf@gmail.com (Josencler L. R. Ferreira);

Instituto de Ciências Biológicas (ICB), Universidade Federal do Rio Grande – FURG, Cx. P. 474, CEP 96200-970, Rio Grande, RS, Brasil

Abstract

Compounds from the nanotechnology industry, such as carbon-based nanomaterials, are strong candidates to contaminate aquatic environments because their production and disposal have exponentially grown in a few years. Previous evidence shows that fullerene C_{60}, a carbon nanomaterial, can facilitate the intake of metals or PAHs both *in vivo* and *in vitro*, potentially amplifying the deleterious effects of these toxicants in organisms. The present work aimed to investigate the effects of fullerene C_{60} in a *Danio rerio* (zebrafish) hepatocyte cell lineage exposed to benzo[a]pyrene (BaP) in terms of cell viability, oxidative stress parameters and BaP intracellular accumulation. Additionally, a computational docking was performed to investigate the interaction of the fullerene C_{60} molecule with the detoxificatory and antioxidant enzyme πGST. Fullerene C_{60} provoked a significant ($p<0.05$) loss in cellular viability when co-exposed with BaP at 0.01, 0.1 and 1.0 µg/L, and induced an increase ($p<0.05$) in BaP accumulation in the cells after 3 and 4 hours of exposure. The levels of reactive oxygen species (ROS) in the cells exposed to BaP were diminished ($p<0.05$) by the fullerene addition, and the increase of the GST activity observed in the BaP-only treated cells was reduced to the basal levels by co-exposure to fullerene. However, despite the potential of the fullerene molecule to inhibit π GST activity, demonstrated by the computational docking, the nanomaterial did not significantly ($p>0.05$) alter the enzyme activity when added to GST purified extracts from the zebrafish hepatocyte cells. These results show that fullerene C_{60} can increase the intake of BaP into the cells, decreasing cell viability and impairing the detoxificatory response by phase II enzymes, such as GST, and this latter effect should be occurring at the transcriptional level.

Keywords: nanotoxicology; BaP; synergistic effect; delivery; GST.

1. Introduction

The fate of products and effluents from the nanotechnology industry has been a growing matter of concern because their production and disposal have exponentially risen in the last few years (Kahru and Dubourguier, 2010). The current data about the actual risks to humans and to the environment are not conclusive, and this is mainly due to the lack of information concerning their mechanisms of toxicity, actual concentrations and chemical behavior in the environment (Christian et al., 2008; Aschberger et al., 2011). However, the novel chemical and physical properties arising from the nanoscale greatly enhance the reactivity of the nanoparticles with biomolecules, making the nanomaterials potentially toxic and capable of harming the environment (Kahru and Dubourguier, 2010). On the other hand, it must also be considered that some works show low toxicity levels of carbon nanomaterials (such as fullerenes) in fish, at least with respect to oxidative stress parameters (Fraser et al., 2011; Henry et al., 2011).

Despite the debate concerning the actual toxicity level of the nanomaterials, especially in the aquatic environment, there is a consensus that nanomaterials may potentially affect biological systems not only *per se*, but also through interaction with other compounds (Christian et al., 2008; Henry et al., 2011). Considering their high reactivity, a question arises about what can happen when nanomaterials are in the presence of other toxic molecules. One of the first attempts to investigate this issue was conducted by Limbach et al. (2007), who measured the oxidative stress in human lung epithelial cells induced by nano-silica doped with a number of metals. This study found higher damage in the treatments with cobalt- and manganese-doped silica nanoparticles than in metals or silica alone. Because nano-silica facilitated the uptake of the metals by the cells, this mechanism was so-called the “Trojan horse” effect. This type of delivery mechanism displayed by nanomaterials has been investigated in a few additional nanotoxicological studies, mainly with metallic nanoparticles. For example, Fan et al. (2011) showed that nano-TiO_2 enhanced copper bioaccumulation and toxicity in the crustacean *Daphnia magna*, even at low nanomaterial concentrations. It was also found that nano-TiO_2 enhanced arsenate toxicity in *Ceriodaphnia dubia*

(Wang et al. 2011) and, when doped with the lanthanide Ce(IV), it caused deformation in the cell morphology of a human hepatocyte cell line (Mao et al. 2010).

Studies investigating co-exposure with carbon-based nanocompounds, such as nanotubes and fullerenes, are less common. Fullerene C_{60} is a worldwide produced nanomaterial with a unique cage-like molecular structure made solely of carbon. Although highly hydrophobic, due to its electronic configuration it can form strong C_{60}-H_2O bonds when in colloidal water suspensions (Andrievsky et al. 2002; Khokhryakov et al. 2006), resulting in stable nano-aggregates that can promote deleterious effects in biological systems (Murdock et al. 2008; Ehrenberg et al. 2009).

C_{60} has been widely investigated in terms of the chemical and physical interactions with a range of molecules and devices looking for applications as nano-probes, nano-sensors and nano-electrodes (Nakashima et al. 1998; Cho et al. 2005; Goyal et al. 2005) and in medicine (Partha et al. 2008; Pinteala et al. 2009; Ganji et al. 2010; Tarabukina et al. 2010; Adini et al. 2011; Santos et al. 2011). Despite being poorly studied, the uptake rate and toxicity of other environmental contaminants seem to be somehow affected when co-exposed to fullerene. Baun et al. (2008) indicated that co-exposure with fullerene C_{60} enhanced the toxicity of phenanthrene to the microcrustacean *Daphnia magna* and to the algae *Pseudokirchneriella subcapitata.* This was due, at least in part, to the high adsorption of phenanthrene molecules onto C_{60} nano-aggregates, which facilitated phenanthrene uptake. Similarly, Costa et al. (2012) observed that arsenic (As^{III}) uptake was higher in zebrafish hepatocytes co-exposed to fullerene (1 mg/L).

Among the polycyclic aromatic hydrocarbons (PAHs), benzo[a]pyrene (BaP) is one of the most important due to its ubiquitous presence in most environments. It is produced mainly during the incomplete combustion of organic matter and in cigarette smoke (Rose and Levi 2004). It is also a carcinogen and mutagen toxicant and reactive oxygen species (ROS) generator (Sasco et al. 2004; Naspinski et al. 2008). Its detoxification process includes metabolization by phase I enzymes that can produce electrophilic epoxides that can readily bind to DNA (Walker et al. 2001). BaP contamination can be harmful through the generation of oxidative stress (Palanikumar et al. 2012),

the inhibition of retinoids synthesis (Alsop et al. 2007) and the formation of DNA adducts (Kurelec et al. 1991). The exposure of cultured cells to BaP can also cause changes in gene expression (Castorena-Torres et al. 2008), oxidative impairment (Winzer et al. 2001) and an increase of the carcinogenic risk by interaction with 17<beta>-estradiol (Chang et al. 2007), among many other deleterious effects.

In order to investigate the influence of fullerene C_{60} upon the toxicity of an important environmental contaminant, such as BaP, the present work aimed to assess the oxidative stress parameters, cell viability and bioaccumulation of BaP in ZF-L cells, an established culture of hepatocytes from the zebrafish *Danio rerio* (Cyprinidae). This cell lineage was chosen because *Danio rerio* is a highly suitable biological model widely used in toxicology, including in studies with nanomaterials (Fako and Furgeson, 2009; Costa et al, 2012). Additionally, an *in silico* study was performed by computational docking to verify the hypothesis of the interaction of the fullerene C_{60} molecule with the antioxidant and phase II detoxificatory enzyme glutathione-S-transferase (GST).

2 Material and Methods

2.1 Preparation of the chemicals

2.1.1 Preparation and characterization of C_{60} suspension

In order to produce a homogeneous suspension of C_{60} nanoparticles, two hundred milligrams of fullerene C_{60} in powder form (99% purity, SES Research - USA) was added to 1 liter of ultra-pure Milli-Q water and stirred for two months under artificial light. After this period, the suspension was centrifuged at 25,000 x g and 15 ºC for 1 hour to remove the bigger aggregates and was then sequentially filtered by 0.45 and 0.20 µm nylon membranes. This methodology was based on the work of Lyon et al. (2006) where no organic solvent was employed because these solvents can release residual degradation products that affect the toxicity of the nanomaterial (Henry et al.,

2007). The concentration of the suspension was determined by measurement of the total organic carbon content in a total organic carbon analyzer (TOC-V CPH – Shimadzu Corp. - Japan). The characterization of the C_{60} suspension was performed by transmission electron microscopy (TEM) in a JEOL JSM 1200 EX II transmission electron microscope operating at 100 kV. For the TEM, aliquots of the C_{60} suspension (10µl) were disposed onto 300 mesh TEM grids (SPI) that were coated with Formvar. The analysis was performed after 24 h to allow sample evaporation, according to previous studies (Britto et al., 2012; Costa et al., 2012; Ferreira et al., 2012). As previously reported for C_{60} suspensions prepared using the water-stirring method without the addition of organic solvents (Lyon et al. 2006; Britto et al., 2012; Costa et al., 2012; Ferreira et al., 2012), the ubiquitous presence of fullerene nano-aggregates in the nanometer range were seen in the C_{60} suspension analyzed by TEM (**Figure 1**).

2.1.2 Preparation of BaP solutions

BaP solutions ranging from 0.01 to 10.00 µg/mL were obtained by dissolving benzo[a]pyrene (Fluka, purity ≥ 96%) in dimethyl sulfoxide (DMSO) (Synth, Brazil). The final concentration of DMSO in contact with the cells was 1% since Filgueira et al. (2007) showed that this DMSO concentration was not deleterious for an erythroleukemic cell line. In addition, the DMSO control group showed no effects in the analyzed variables (see **Results**).

2.2 Maintenance of the hepatocytes

Zebrafish hepatocytes (ZF-L lineage) purchased from the American Type Culture Collection (ATTC) were maintained in culture flasks with 10 mL of RPMI 1640 (Gibco) medium supplemented with 10% fetal bovine serum and a 1% antibiotic/antimycotic cocktail (streptomycin, amphotericin and penicillin) at 28 °C. For the exposure assays, cells were initially removed from the flasks with 0.125% trypsin, washed with phosphate buffered saline (PBS) and transferred to 24-well culture plates (0.5 mL per well, 10^6 cells/mL) to settle down and adhere. After 24h, the cells

were carefully washed with PBS and exposed to the treatments.

2.3 Experimental design and procedure

All exposures were performed with at least 10^6 cells/mL in a final volume of 400 µl per well (toxicants or vehicles plus RPMI medium), with four wells per treatment at 28 °C over 4 h. After this period, the cells were washed with PBS to remove the toxicants, and the estimation of the number of cells was performed, as well as the cell viability assay (see next section). Initially, some assays were conducted with a range of concentrations of both C_{60} (0.1, 1.0 and 10.0 mg/L) or BaP alone (from 0.01 to 10.0 µg/L) in order to determine the optimal concentrations for which the cell viability was not altered. Because none of the fullerene concentrations altered the cell viability (see **Results** section) and considering previous exposure studies (Costa et al. 2012), the concentration of 1.00 mg/L of C_{60} was chosen for the further co-exposures with BaP. BaP concentrations of 0.01, 0.10 and 1.0 µg/L were chosen for the subsequent exposures because they did not impair hepatocyte viability. Control groups included a Milli Q water control (the solvent of the fullerene suspensions) and a DMSO control (BaP solvent) at a final concentration of 1%.

2.4 Estimation of number of cells and viability assays

Four control wells (800 µl of cell suspension) from the 24-well plate were pooled and diluted with RPMI medium to obtain aliquots of 100%, 75%, 50% and 25% of the original cell suspension. After that, the cells were counted in an optical light microscope, and 200 µl of the dilutions were read in duplicate at 630 nm with an ELISA microplate reader (Biotek Elx 800). The absorbance values were then fitted to the respective number of cells previously counted in the microscope, and a standard curve was made to estimate the number of cells of the treatments after reading at 630 nm (Costa et al. 2012).

The technique of intracellular reduction of 2-(4,5-dimethyl-2-thiazolyl)-3,5-diphenyl-2H-tetrazolium bromide (MTT) to formazan by mitochondrial dehydrogenase activity was employed

for the cell viability measurement. Aliquots of 20 µl of cell suspensions were added in 96-well plates and incubated for 30 min in the dark at 28 ºC with 20 µl of a 12 mM MTT solution. Following the incubation, the plate was centrifuged for 7 min at 1,100 rpm, the supernatant was discarded and 200 µl of DMSO was added to dissolve the blue formazan crystals. Finally, the samples were read at 490 nm in an ELISA microplate reader. The absorbance values were considered as a measure of dehydrogenase functionality and, therefore, an indirect cell viability parameter (Costa et al. 2012).

2.5 Determination of the ROS concentration

Following the exposure, the hepatocytes were centrifuged at 600 x g for 5 min at 10 ºC, the supernatant was discarded and the cells were re-suspended in a solution with 40 µM of the fluorescent probe 2,7′dichlorodihydrofluorescein diacetate (H_2DCF-DA, Invitrogen) in PBS. Immediately, the cell suspension was transferred to a white 96-well microplate (160 µl per well in triplicate) and read in a microplate reader fluorimeter (Victor 2, Perkin Elmer) at wavelengths of 485 and 520 nm for the excitation and emission, respectively. The ROS concentration was expressed in terms of fluorescence area resulting from the integration of the fluorescence values between 0 and 70 min after fitting to a second order polynomial. The ROS area was fitted to the estimated cells number in each treatment (Costa et al. 2012).

2.6 Glutathione-S-transferase (GST) activity assay

The activity of the phase II enzyme GST was determined through the monitoring of a conjugate formed by 1 mM of reduced glutathione (GSH) and 1 mM of 1-chloro-2,4-dinitrobenzene (CDNB) (Sigma) in the presence of 100 µl of cell extract in PBS at 340 nm (Habig and Jakoby, 1981). The results were expressed as nanomoles of GSH-CDNB conjugate/min/mg protein at 25 °C and pH 7.40. The total protein content was assessed through a commercial kit (Doles, Brazil) based on the pirogalol method.

209

210 **2.7 Quantification of the BaP concentration in the BaP working solutions**

211 The PAH analyses were conducted using a gas chromatograph coupled with a mass
212 spectrometer (Perkin Elmer® Clarus 500 – GC-MS) and equipped with an Elite-5MS silica capillary
213 column (Perkin Elmer® 5% phenyl-95% methylpolysiloxane; 30 m x 0.25 mm, 0.25 µm film
214 thickness). The injector was kept at 280 °C in splitless mode. The temperature program started at 40
215 °C, increased at a rate of 10 °C min^{-1} to 60 °C, then increased at 5 °C min^{-1} to 290 °C, was
216 maintained at 290 ºC for 5 minutes and then increased at 10 °C min^{-1} to 300 °C and was held
217 constant for 10 minutes. Helium was used as the carrier gas (1.5 mL min^{-1}). The MS operating
218 conditions were: interface at 290 °C, ion source at 200 °C and electron energy of 70 eV. The data
219 were acquired under selected ion monitoring (SIM) mode. Compound identification was based on
220 the individual mass spectra and the GC retention time in comparison to literature, library data, and
221 authentic standards. Standards were injected and analyzed under the same conditions as the
222 samples. The limit of detection (LOD) of BaP was in the range of 1.75 ng mL^{-1}, and the limit of
223 quantification (LOQ) was 5 ng mL−1. The procedure was checked for recovery efficiencies by
224 analyzing uncontaminated samples spiked with BaP standards. The average recoveries (n=5) ranged
225 from 88% to 101%. PAH surrogate standards (p-therphenyl-d14) were added to all samples to
226 monitor the procedures of sample extraction, recovery and analysis. The average recoveries of the
227 surrogate standards added samples varied from 91 % to 117%. One laboratory blank and one
228 duplicate were run with every 10 samples. The coefficient of variation of the BaP concentrations in
229 the duplicates was less than 15%. Still, to evaluate the precision of the analysis, two replicates of
230 the samples were analyzed. The relative standard deviation (RSD) of the replicates varied between
231 2 and 5%. Regular analyses of the reference material from the International Atomic Energy Agency
232 Analytical Quality Control Services (Organic Contaminants in Marine Sediment - IAEA-417) and
233 semiannual participation in the intercomparison exercises promoted by the Canadian Association
234 for Laboratory Accreditation (CALA) have shown satisfactory quality control. The measured

concentrations confirmed that the nominal concentration (1,000 ng/mL) was within 1,018±30.0 ng/mL.

2.8 Estimation of BaP intracellular accumulation

The BaP (or its metabolites) intracellular accumulation (1.0 μg/L) over time (1, 2, 3 and 4 h of incubation) with and without co-exposure to C_{60} (1.0 mg/L) was assessed following the protocol described by Filgueira et al. (2007). The readings were performed after washing the cells with PBS, and aliquots of 160 μL were put in a white 96-well plate to read in a fluorimeter at the wavelengths of 340 and 450 nm for excitation and emission, respectively.

2.9 *In silico* assay of the interaction of fullerene C_{60} molecule with π GST

Due to the results obtained in the GST activity assay (see **Results** section), a mathematical simulation (computational docking) of the interaction between the molecules of C_{60} and GST was performed to investigate the potential affinity of the fullerene C_{60} for GST enzyme, which could interfere with the enzymatic activity. For this simulation, the class pi mitochondrial GST (π GST) was chosen as the model for the C_{60} docking. This isoform was selected due to the high number of mitochondria present in hepatocytes, the availability of computational data from a mouse liver π GST, which possess a good analogy with the zebrafish π GST, and the recent evidence of the role of π GST in BaP detoxification in zebrafish (Garner and Di Giulio, 2012). The docking simulations of the fullerene with mouse liver π GST complexed with S-(P-nitrobenzyl) glutathione (PDB code 1GLQ) were performed using AutoDock Vina 1.1.1 [1] followed by redocking with AutoDock 4.0.1. Before the simulations, the inhibitor S-(P-nitrobenzyl) glutathione was removed from the structure, and the enzyme was geometrically optimized using the Universal Force Field (UFF) implemented in the Avogadro 0.9 software. The fullerene molecule was constructed in Avogadro, and its geometry was optimized using UFF. The enzyme was kept in its catalytic (dimeric) form. AutoDock Tools was used to create the inputs in the .pdbqt format for the simulations in AutoDock

Vina. A second docking was made using AutoDock to confirm the data obtained by AutoDock Vina. The entire system was considered for the simulations. The grid box was centralized at the coordinates x = 63.504, y = 18.195 and z = 5.743, with dimensions of 60, 60 and 60 Å using a spacing of 1 Å and the exhaustiveness set to 50. All other parameters were used as defaults. The conformation with the lowest binding free energy was accepted as the best affinity model. The conformations and interactions were analyzed using the software Accelrys Discovery Studio Visualizer 2.5 and PyMOL. A redocking was conducted using the S-(P-nitrobenzyl) glutathione to validate the method. In this case, the molecule was successfully positioned at a similar position to the crystallographic conformation, with an RMSD less than 1.

2.10 Verification of the effect of C_{60} on the activity of GST in purified extracts

Based on the results from the docking assay, and in order to investigate whether the modulation of GST activity observed in the treatments BaP+C_{60} was induced by the direct interaction of the nanomaterial with the enzyme (see **Results** section), an *in vitro* assay was run in which the GST activity was measured in GST purified extracts previously exposed to C_{60}. The purified extracts of GST from ZF-L cells were obtained through a commercial kit (MagneGST®, Promega), and the procedure was followed according to manufacturer's instructions. The method is based on the binding of glutathione-conjugated magnetic particles with GST enzymes present in the samples, which allows for the separation of these enzymes from the rest of the cellular extract. Once the purified extracts were obtained, an exposure assay was performed in which the GST extracts were mixed with 10 mg/L fullerene C_{60} over 4 h at 28 ºC in the absence of light. After the exposure, a GST activity assay was performed identically to the method described in **Section 2.6**.

2.11 Statistical analysis

Data from all assays were analyzed by means of ANOVA (Zar, 1984) after the verification of normality and homogeneity of variances; if even one of the assumptions was violated, mathematical

transformations were applied. Post-hoc comparisons among the treatments were performed through the Newmann-Keuls method, and a significance level of 0.05 was adopted for all steps of the analysis.

3 Results

Because the cell viability was not significantly ($p>0.05$) reduced by any of the three tested C_{60} aggregates (**Figure 2a**), and based on previous evidence of oxidative balance disturbance in fish, both *in vivo* (Oberdörster 2004) and in ZF-L cultured cells (Costa et al. 2012), a concentration of 1.0 mg/L was adopted for the subsequent co-exposures with BaP. BaP, however, was capable of reducing cell viability ($p<0.05$) at 10.0 μg/L (**Figure 2b**), thus the concentrations of 0.01, 0.1 and 1.0 μg/L were chosen for co-exposure to C_{60}. At those BaP concentrations, fullerene C_{60} significantly ($p<0.05$) lowered the cell viability during co-exposure experiments (**Figure 3**).

The exposure to 1.00 μg/L of BaP resulted in an augmented intracellular accumulation of BaP (or its metabolites) in ZF-L cells only when co-exposed to fullerene C_{60} (**Figure 4a).** The longer the incubation time was, the higher the accumulation values ($p<0.05$). **Figure 4b** shows the fluorescence units in the blank samples (without cells), demonstrating that C_{60} did not interfere ($p>0.05$) with the readings at the wavelengths used for the BaP accumulation measurements.

Figure 5 shows the levels of intracellular ROS of the exposed ZF-L cells. The BaP-only treatments did not significantly ($p>0.05$) increase the ROS generation when compared to the respective controls. On the contrary, the co-exposure with C_{60} decreased ($p<0.05$) the basal ROS level.

The activity of the phase II enzyme GST increased ($p<0.05$) after exposure to 0.10 and 1.00 μg/l of BaP **(Figure 6)**. However, the co-exposure to C_{60} reversed the GST activity to its basal levels despite the presence of BaP.

Figure 7 shows a 3D representation from the docking simulation of the C_{60} in the π GST

313 molecule. The results showed that the fullerene C_{60}, in its more stable conformation (Gibbs free
314 energy: -11.5 kcal/mol), was situated at a region of the enzyme postulated as the binding site of
315 HEPES, near the C-terminal region between the elements β2 and α1. This region, due to the
316 presence of the amino acids Arg18, Ala22, Trp28 and Phe192, produces a hydrophobic surface that
317 favors fullerene binding stabilization through Van der Waals forces (Figure 7b). Moreover, the data
318 revealed that fullerene acts via three cation-π type interactions with the residual Lys188, and such
319 interactions seem to be the main force contributing to the affinity of the nanomaterial with the
320 HEPES binding site of π GST.
321 The exposure of the ZF-L purified extracts to 10 mg/L of C_{60} for 4 h had no effect on the
322 GST activity ($p>0.05$). The Control groups produced 12.95 ± 4.38 nanomoles of GSH-CDNB
323 conjugate/min/mg protein, whereas the C_{60} groups produced 14.13 ± 4.22 nanomoles of GSH-
324 CDNB conjugate/min/mg protein.
325
326 **4 Discussion**
327 Fullerene toxicity is a controversial issue. Kahru and Dubourguier (2010) compiled fullerene
328 toxicological data for fourteen organisms and classified this nanomaterial as very toxic, taking into
329 account the lowest median L(E)C_{50} values for all test organisms. However, some studies indicate
330 the absence of fullerene toxicity (i.e., Xia et al. 2010), whereas others considered that ROS
331 generation by aqueous fullerene suspension is minimal (i.e., Henry et al., 2011). Recently, Trpkovic
332 et al. (2012) stated that fullerene toxicity can be elicited by ROS-dependent (when photo-excited)
333 and ROS-independent mechanisms, where the latter is considered to be through cell membrane
334 damage and/or induction of autophagy. An ROS-independent pathway should be considered
335 responsible for the cytotoxicity observed in the present study because fullerene and BaP exposures
336 were performed in incubators in the dark at 28 ^{o}C.
337 Yang et al. (2010) raised the possibility of aqueous fullerene suspensions acting similarly to
338 dissolved organic matter (DOM), changing the bioavailability of toxic molecules (such as PAH).

339 This concept was related to the ‘Trojan horse’ paradigm first postulated by Limbach et al. (2007). In
340 addition, Henry et al. (2011) highlighted the potential environmental risk of fullerene due to its
341 capacity to act as a carrier for other contaminants. However, the “Trojan horse’ concept needs to be
342 better studied. The original paper of Limbach et al. (2007) compared the levels of intracellular ROS
343 between silica nanoparticles containing metals and the corresponding oxides. Other authors, such as
344 Baun et al. (2008), considered the “Trojan horse’ effect under the view of the augmented
345 accumulation of a toxic molecule (as phenanthrene) when co-exposed with a nanomaterial, such as
346 fullerene, and the toxicological consequences of this co-exposure. The same concept was
347 considered by Sun et al. (2009), in terms of arsenic accumulation in carp gills after co-exposure
348 with titanium dioxide nanoparticles, and by Costa et al. (2012) studying arsenic accumulation in
349 zebrafish hepatocytes after co-exposure to fullerene. Following the postulation of Baun et al.
350 (2008), the present work demonstrated the deleterious effects and higher accumulation of BaP (or
351 its metabolites) when co-exposed with fullerene C_{60} and the consequences in terms of cytotoxicity,
352 intracellular ROS and detoxification capacity.

353 The effects of mixtures of pollutants in the environment are usually hard to predict due to
354 many factors. This task is even more difficult when nanomaterials are under study in virtue of their
355 inherent properties, which can amplify or alleviate the toxic effects of other compounds. To the best
356 of our knowledge, information about the influence of the physical-chemical characteristics of toxic
357 molecules on nanomaterial interactions is currently lacking. Fullerene C_{60} has induced loss in cell
358 viability when co-exposed with BaP, which did not occur with cells treated with BaP only (**Figure**
359 **3**). This result is probably due to the increase of the BaP intracellular accumulation caused by
360 fullerene C_{60} (**Figure 6)**. Once a higher BaP concentration is inside the cells, the increasing damage
361 may lead to the observed loss in the mitochondrial dehydrogenase functionality, as measured by the
362 MTT assay. This finding is in accordance with the work of Baun et al. (2008), as mentioned above.
363 Al-Subiai et al. (2012) registered higher genotoxicity in mussel haemocytes when fluoroanthene
364 and fullerene were co-exposed. However, this is not always true. Yan et al. (2010) reported lower

365 histological damage induced by fluoroanthene when co-exposed with fullerene under UV radiation,
366 and Baun et al. (2008) observed that fullerene did not influence the toxicity of atrazine and methyl
367 parathion to the algae *P. subcapitata* and the crustacean *D. magna*.

368 The presence of fullerene C_{60} reduced the intracellular concentration of ROS (**Figure 4**),
369 resulting in an antioxidant effect. This may be due to the low number of viable cells in BaP+C_{60}
370 treatments or to the ability to react with radicals, which is attributed to the C_{60} molecule
371 (Andrievsky et al. 2009; Xia et al. 2010). This property is postulated as a non-stoichiometric
372 reaction, in which a self-neutralization could occur when the molecule is in a hydrated state, and it
373 could give the observed scavenging characteristics to the nanomaterial (Andrievsky et al. 2009).
374 Previous studies from our group employing cell suspension from carp *Cyprinus carpio* brains
375 registered a reduction of intracellular ROS after 2 h of exposure to 1 mg/L of fullerene, also
376 showing an antioxidant behavior of an aqueous suspension of this nanomaterial (Acosta et al.,
377 2012).

378 The activity of the total GST was raised in the BaP-only treatments, which is a classical
379 effect of this PAH and is associated to the generation of ROS (Vieira et al. 2008; Palanikumar et al.
380 2012). Interestingly, co-exposure to C_{60} hinders this increase, keeping the enzyme activity at the
381 basal levels (**Figure 6**), a result that can be deleterious for cell viability (as observed) because of the
382 lowering of the detoxifying capacity. Moreover, the computational docking showed that the C_{60}
383 molecule can potentially affect the GST activity because of its affinity for a hydrophobic region of π
384 GST, which is postulated as an allosteric site of HEPES. Such interaction may alter the C terminal
385 region of the enzyme, producing conformational changes that can modify the xenobiotic binding
386 site (Ji et al. 1997). From a toxicological point of view, this evidence is relevant because it
387 demonstrates that fullerene C_{60} can induce deleterious effects by impairing important detoxificatory
388 responses, such as the phase II mechanisms.

389 However, the nanomaterial did not affect the enzyme activity in the GST purified extracts of
390 ZF-L cells, even at a concentration of 10 mg/l. A possible explanation is that, although the molecule

of fullerene has the potential to inhibit π GST activity, it could not bind to the allosteric site of HEPES due to the nanoparticle size, which is a consequence of the aggregation state of fullerene (an aspect not considered in the docking analysis). The lack of effects in the purified extracts in terms of the inhibition of GST activity contrasts with the cell assays, where a clear inhibition of this enzyme was observed, suggesting that the deleterious effects of fullerene may be occurring at the transcriptional level. Schlenk et al. (2008) stated that GST enzymes are more abundant in the liver, being the π-class homolog the predominant form in cyprinids. In this way, although 1-chloro-2,4-dinitrobenzene (CDNB) is a substrate for several GST isoforms (Schlenk et al., 2008), it is expected that the measured activity should reflect the catalytic activity of the π isoform when measured in zebrafish hepatocytes.

Mashino et al. (2001) proved in a previous study that fullerene functionalized with carboxylic groups inhibited glutathione reductase, another enzyme that has glutathione as co-substrate. Thus, both the agglomeration of fullerene molecules in the aqueous suspension and the fact that the nanomaterial was in a non-functionalized form should explain the lack of inhibitory potency in the assays with purified extracts and suggests indirect toxicity mechanism(s). At the present, the hypothesis of the role of the fullerene as a down-regulator of GST transcription is being analyzed at our laboratory.

5 Conclusions

Altogether, the results show that fullerene elicited toxic effects in ZF-L cells by increasing the intake of BaP, decreasing cell viability and impairing the detoxificatory response by the phase II enzyme GST. This latter effect probably occurs at the transcriptional level. The potential affinity of fullerene to π GST needs further investigation, since this isoform is postulated as the predominant GST class in cyprinids.

Conflict of interest statement

The authors declare that there are no actual or potential conflicts of interest in the present work.

Acknowledgments

The Brazilian National Research Council sponsored J. L. Ribas Ferreira with a graduate fellow (CNPq No 553753/2009-6), J.M. Monserrat (PQ No 306027/2009-7) and G. Fillmann (CNPq PQ No 314335/2009-9) with a productivity research fellowship, and N. Maxmilla and T. A. França with an undergraduate fellow (CNPq PIBIC Program). The logistic and material support from the *Instituto Nacional de Ciência e Tecnologia de Nanomateriais de Carbono* (INCT-Nano CNPq) and the Electronic Microscopy Center, at the *Universidade Federal do Rio Grande do Sul* (UFRGS), were essential for the execution of the present study. The support of DECIT/SCTIE-MS through the Brazilian National Research Council (CNPq) and *Fundação de Amparo à Pesquisa do Estado do Rio Grande do Sul* (FAPERGS, Proc. 10/0036-5–PRONEX/Conv. 700545/2008; Proc. 11/1348-0-Edital 002/2011 PQG) is also acknowledged. The present study was supported by the Nanotoxicology Network (MCTI/CNPq process number 552131/2011-3). Financial support from ANPCyT-PICT RAICES (process number 35913) is acknowledged by F.R. de la Torre and J.M. Monserrat.

REFERENCES

Acosta, D.S., Kneip, F.C., Alves de Almeida, E., Ventura-Lima, J., Monserrat, J.M., Geracitano, L.A., 2012. Fullerene and omega-3 and omega-6 fatty acids on fish brain antioxidant status. Fish Physiology and Biochemistry. 38, 1477-1485.

Adini, A.R., Redlich, M., Tenne, R., 2011. Medical applications of inorganic fullerene-like nanoparticles. Journal of Materials Chemistry. 21, 15121.

Alsop, D., Brown, S., Van Der Kraak, G., 2007. The effects of copper and benzo[a]pyrene on retinoids and reproduction in zebrafish. Aquatic Toxicology. 82, 281-95.

Al-Subiai, N., Arlt, V.M., Frickers, P.E., Readman, J.W., Stolpe, B., Lead, J.R., Moody, A.J., Jha, A.N., 2012. Merging nano-genotoxicology with eco-genotoxicology: An integrated approach to determine interactive genotoxic and sub-lethal toxic effects of C_{60} fullerenes and fluoranthene in marine mussels, *Mytilus* sp. Mutation Research. 745, 92-103.

Andrievsky, G.V., Klochkov, V.K., Bordyuh, A.B., Dovbeshko, G.I., 2002. Comparative analysis of two aqueous-colloidal solutions of C_{60} fullerene with help of FTIR reflectance and UV–Vis spectroscopy. Chemical Physics Letters. 364, 8-17.

Andrievsky, G.V, Bruskov, V.I., Tykhomyrov, A.A, Gudkov, S.V., 2009. Peculiarities of the antioxidant and radioprotective effects of hydrated C_{60} fullerene nanostuctures *in vitro* and *in vivo*. Free Radical Biology & Medicine. 47, 786–93.

Aschberger, K., Micheletti, C., Sokull-Klüttgen, B., Christensen, F.M., 2011. Analysis of currently available data for characterising the risk of engineered nanomaterials to the environment and human health - Lessons learned from four case studies. Environment International. 37, 1143-1156.

Baun, A., Sørensen, S. N., Rasmussen, R.F., Hartmann, N.B., Koch, C.B., 2008. Toxicity and bioaccumulation of xenobiotic organic compounds in the presence of aqueous suspensions of aggregates of nano-C_{60}. Aquatic Toxicology. 86, 379-387.

Britto, R.S., Garcia, M.L., da Rocha, A.M., Flores, J.A., Pinheiro, M.V.B., Monserrat, J.M., Ferreira, J.L.R., 2012. Effects of carbon nanomaterials fullerene C_{60} and fullerol C_{60} $(OH)_{18–22}$ on gills of fish *Cyprinus carpio* (Cyprinidae) exposed to ultraviolet radiation. Aquatic Toxicology. 114-115, 80-87.

Castorena-Torres, F., De León, M., Cisneros, B., Zapata-Perez, O., Salinas, J., Albores, A., 2008. Changes in gene expression induced by polycyclic aromatic hydrocarbons in the human cell lines HepG2 and A549. Toxicology *in Vitro*. 22, 411-421.

Chang, L. W., Chang, Y.-Ching, Ho, C.-Chi, Tsai, M.-Hsien, Lin, P., 2007. Increase of carcinogenic risk via enhancement of cyclooxygenase-2 expression and hydroxyestradiol accumulation in human lung cells as a result of interaction between BaP and 17-beta estradiol. Carcinogenesis. 28, 1606-12.

Cho, Y.-J., Ahn, T.K., Song, H., Kim, K.S., Lee, C.Y., Seo, W.S., Lee, K., Kim, S.K., Kim, D., Park, J.T., 2005. Unusually high performance photovoltaic cell based on a [60]fullerene metal cluster-porphyrin dyad SAM on an ITO electrode. Journal of the American Chemical Society. 127, 2380-1.

Christian, P., Von der Kammer, F., Baalousha, M., Hofmann, Th., 2008. Nanoparticles: structure, properties, preparation and behaviour in environmental media. Ecotoxicology. 17, 326-343.

Costa, C.L.A., Chaves, I.S., Ventura-Lima, J., Ferreira, J.L.R., Ferraz, L., Carvalho, L.M.D., Monserrat, J.M., 2012. *In vitro* evaluation of co-exposure of arsenium and an organic nanomaterial (fullerene, C_{60}) in zebrafish hepatocytes. Comparative Biochemistry and Physiology. C 155, 206-212.

Ehrenberg, M.S., Friedman, A.E., Finkelstein, J.N., Oberdörster, G., McGrath, J.L., 2009. The

494 influence of protein adsorption on nanoparticle association with cultured endothelial cells.
495 Biomaterials. 30, 603–610.
496
497 Fako, V.E., Furgeson, D.Y., 2009. Zebrafish as a correlative and predictive model for assessing
498 biomaterial nanotoxicity. Advanced Drug Delivery Reviews. 61, 478-86.
499
500 Fan, W., Cui, M., Liu, H., Wang, C., Shi, Z., Tan, C., Yang, X., 2011. Nano-TiO_2 enhances the
501 toxicity of copper in natural water to *Daphnia magna*. Environmental Pollution. 159, 729-734.
502
503 Ferreira, J.R.F., Barros, D.M., Geracitano, L.A., Fillmann, G., Fossa, C.E., De Almeida, E.A.,
504 Prado, M.C., Neves, B.R.A., Pinheiro, M.V.B., Monserrat, J.M., 2012. Influence of *in vitro*
505 exposure to fullerene C_{60} in redox state and lipid peroxidation of brain and gills of carp *Cyprinus*
506 *carpio* (Cyprinidae). Environmental Toxicology and Chemistry. 31, 961–967.
507
508 Filgueira, D.M.V.B., de Freitas, P.S., Souza Votto, A.P., Fillmann, G., Monserrat, J.M., Geracitano,
509 L.A., Trindade, G.S., 2007. Photodynamic action of benzo[a]pyrene in K562 cells. Photochemistry
510 and Photobiology. 83, 1-6.
511
512 Fraser, T.K, Reinardy, H,C., Shaw, B.J., Henry, T.B., Handy, R.D., 2011. Dietary toxicity of single-
513 walled carbon nanotubes and fullerenes (C_{60}) in rainbow trout (*Oncorhynchus mykiss*).
514 Nanotoxicology. 5(1), 98-108.
515
516 Ganji, M.D., Yazdani, H., Mirnejad, A., 2010. $B_{36}N_{36}$ fullerene-like nanocages: A novel material for
517 drug delivery. Physica E: Low-dimensional Systems and Nanostructures. 42, 2184-2189.
518
519 Garner, L.V.T., Di Giulio, R.T., 2012. Glutathione transferase pi class 2 (GSTp2) protects against

520 the cardiac deformities caused by exposure to PAHs but not PCB-126 in zebrafish embryos.
521 Comparative Biochemistry and Physiology. C 155, 573–9.
522
523 Goyal, R.N., Gupta, V.K., Sangal, A., Bachheti, N., 2005. Voltammetric determination of uric acid
524 at a fullerene-C_{60}-modified glassy carbon electrode. Electroanalysis. 17, 2217-2223.
525
526 Habig, W.H., Jakoby, W.B., 1981. Assays for differentiation of glutathione S-transferases. Methods
527 in Enzymology. 77, 398–405.
528
529 Henry, T.B., Menn, F.M., Fleming, J.T., Wilgus, J., Compton, R.N., Sayler, G.S., 2007. Attributing
530 effects of aqueuous C_{60} nano-aggregates to tetrahydrofuran decomposition products in larval
531 zebrafish by assessment of gene expression. Environmental Health Perspectives. 115, 1059-1065.
532
533 Henry, T.B., Petersen, E.J., Compton, R.N., 2011. Aqueous fullerene aggregates (nC_{60}) generate
534 minimal reactive oxygen species and are of low toxicity in fish: A revision of previous reports.
535 Current Opinion in Biotechnology. 22, 533-537.
536
537 Ji X., Tordova, M., O'Donnell, R., Parsons J.F., Hayden, J.B., Gilliland G.L., Zimniak, P., 1997.
538 Structure and function of the xenobiotic substrate-binding site and location of a potential non-
539 substrate-binding site in a class π glutathione *S*-transferase. Biochemistry. 36, 9690-9702.
540
541 Kahru, A., Dubourguier, H.-C., 2010. From ecotoxicology to nanoecotoxicology. Toxicology. 269,
542 105-19.
543
544 Khokhryakov, A., Avdeev, M., Aksenov, V., Bulavin, L., 2006. Structural organization of colloidal
545 solution of fullerene C_{60} in water by data of small angle neutron scattering. Journal of Molecular

546 Liquids. 127, 73-78.
547
548 Kurelec, B., Krca, S., Garg A., Gupta, R.C., 1991. The potential of carp to bioactivate
549 benzo[a]pyrene metabolites that bind to DNA. Cancer Letters. 57, 255-260.
550
551 Limbach, L.K., Wick, P., 2007. Exposure of engineered nanoparticles to human lung epithelial cells:
552 Influence of chemical composition and catalytic activity on oxidative stress. Environmental Science
553 & Technology. 41, 4158-4163.
554
555 Lyon, D.Y., Adams, L.K., Falkner, J.C., Alvarez, P.J.J., 2006. Antibacterial activity of fullerene
556 water suspensions: Effects of preparation method and particle size. Environmental Science &
557 Technology. 40, 4360-4366.
558
559 Mao, J., Wang, L., Qian, Z., Tu, M., 2010. Uptake and cytotoxicity of Ce(IV) doped TiO_2
560 nanoparticles in human hepatocyte cell line L02. Journal of Nanomaterials. 2010, 1-8.
561
562 Mashino, T., Okuda, K., Hirota, T., Hirobe, M., Nagano, T., Mochizuki, M., 2001. Inhibitory effects
563 of fullerene derivatives on glutathione reductase. Fullerene Science and Technology. 9, 191-196.
564
565 Murdock, R.C., Braydich-Stolle, L., Schrand, A.M., Schlager, J.J., Hussain, S.M., 2008.
566 Characterization of nanomaterial dispersion in solution prior to *in vitro* exposure using dynamic
567 light scattering technique. Toxicological Sciences. 101, 239–253.
568
569 Nakashima, N., Tokunaga, T., Nonaka, Y., Nakanishi, T., Murakami, H., Sagara, T., 1998. A
570 fullerene/lipid electrode device: Reversible electron transfer reaction of C_{60} embedded in a cast film
571 of an artificial ammonium lipid on an electrode in aqueous solution. Angewandte Chemie

572 International Edition. 37, 2671-2673.
573
574 Naspinski, C., Gu, X., Zhou, G.-D., Mertens-Talcott, S.U., Donnelly, K.C., Tian, Y., 2008. Pregnane
575 X receptor protects HepG2 cells from BaP-induced DNA damage. Toxicological Sciences. 104, 67-
576 73.
577
578 Oberdörster, E., 2004. Manufactured nanomaterials (fullerenes, C_{60}) induce oxidative stress in the
579 brain of juvenile largemouth bass. Environmental Health Perspectives. 112, 1058-1062.
580
581 Palanikumar, L., Kumaraguru, A.K., Ramakritinan, C.M., Anand, M., 2012. Biochemical response
582 of anthracene and benzo[a]pyrene in milkfish *Chanos chanos*. Ecotoxicology and Environmental
583 Safety. 75, 187-97.
584
585 Partha, R., Mitchell, L.R., Lyon, J.L., Joshi, P.P., Conyers, J.L., 2008. Buckysomes: fullerene-based
586 nanocarriers for hydrophobic molecule delivery. ACS Nano. 2, 1950-8.
587
588 Pinteala, M., Dascalu, A., Ungurenasu, C., 2009. Binding fullerenol $C_{60}(OH)_{24}$ to dsDNA.
589 International Journal of Medicine. 4, 193-199.
590
591 Rose, R.L., Levi, P.E., 2004. Reactive Metabolites, in: Ernest Hodgson (ed), A textbook of modern
592 toxicology. John Wiley & Sons, Inc., Hoboken, New Jersey. p. 158.
593
594 Sasco, A.J., Secretan, M.B., Straif, K., 2004. Tobacco smoking and cancer: A brief review of recent
595 epidemiological evidence. Lung Cancer. 45(Suppl. 2), S3–9.
596
597 Santos, L.J., Gonçalves, A.S.P., Krambrock, K., Pinheiro, M.V.B., Eberlin, M.N., Vaz, B.G., de

598 Freitas, R.P., Alves, R.B., 2011. Synthesis of [60]fullerene derivatives bearing five-membered
599 heterocyclic wings and an investigation of their photophysical kinetic properties. Journal of
600 Photochemistry and Photobiology A: Chemistry. 217, 184-190.
601
602 Sun, H., Zhang, X., Zhang, Z., Chen, Y., Crittenden, J.C., 2009. Influence of titanium dioxide
603 nanoparticles on speciation and bioavailability or arsenite. Environmental Pollution. 157, 1165-
604 1170.
605
606 Tarabukina, E., Zoolshoev, Z., Melenevskaya, E., Budtova, T., 2010. Delivery of fullerene-
607 containing complexes via microgel swelling and shear-induced release. International Journal of
608 Pharmaceutics. 384, 9-14.
609
610 Trpkovic, A., Todorovic-Markovic, B., Trajkovic, V., 2012. Toxicity of pristine versus
611 functionalized fullerenes: mechanisms of cell damage and the role of oxidative stress. Archives of
612 Toxicology. 86, 1809-1827.
613
614 Walker, C.H.S., Hopkin, P., Sibly, R.M., Peakall, D.B., 2001. Principles of Ecotoxicology, second
615 edition. Taylor & Francis Inc. New York.
616
617 Wang, D., Hu, J., Irons, D.R., Wang, J., 2011. Synergistic toxic effect of nano-TiO2 and As(V) on
618 *Ceriodaphnia dubia*. Science of the Total Environment. 409, 1351–1356.
619
620 Winzer, K., Winston, G.W., Becker, W., Van Noorden, C.J., Köehler, A., 2001. Sex-related responses
621 to oxidative stress in primary cultured hepatocytes of European flounder (*Platichthys flesus* L.).
622 Aquatic Toxicology. 52, 143-55.
623

624 Vieira, L.R., Sousa, A., Frasco, M.F., Lima, I., Morgado, F., Guilhermino, L., 2008. Acute effects of
625 benzo[a]pyrene, anthracene and a fuel oil on biomarkers of the common goby *Pomatoschistus*
626 *microps* (Teleostei, Gobiidae). The Science of the Total Environment. 395, 87–100.
627
628 Xia, X.R., Monteiro-Riviere, N.A, Riviere, J.E., 2010. Intrinsic biological property of colloidal
629 fullerene nanoparticles (nC_{60}): Lack of lethality after high dose exposure to human epidermal and
630 bacterial cells. Toxicology Letters. 197, 128–34.
631
632 Yang, X.Y., Edelmann, R.E., Oris, J.T., 2010. Suspended C_{60} nanoparticles protect against short-
633 term UV and fluoranthene photo-induced toxicity, but cause long-term damage in *Daphnia magna*.
634 Aquatic Toxicology. 100, 202-210.
635
636 Zar. J. H., 1984. Biostatistical analysis. New Jersey: Prentice Hall.
637

638 **Figure Captions**

639

640 **Figure 1.** Transmission electron microscopy (TEM) image of fullerene C_{60} from the suspension
641 obtained by the solvent-free method.

642

643 **Figure 2.** Cell viability measurement after 4 h of exposure employing the method of reduction of
644 MTT by mitochondrial dehydrogenases. **C**: Milli Q water control. **D**: dimethyl sulfoxide (DMSO)
645 control. **(a)** Percentage of viable cells exposed to fullerene C_{60} (0.1, 1.0 or 10.0 mg/L). **(b)**
646 Percentage of viable cells exposed to BaP (0.01, 0.1, 1.0, or 10.0 µg/L). N= 4 to 16 independent
647 experiments.

648

649 **Figure 3**. Absorbance values of MTT reduction in cells treated with BaP (0.01, 0.10 or 1.0 µg/L)
650 with or without fullerene C_{60} (1.0 mg/L). **C**: Milli Q water control. **D**: dimethyl sulfoxide (DMSO).
651 Same letters indicate the absence of statistically significant ($p>0.05$) differences. N= 4 to 8
652 independent experiments.

653

654 **Figure 4.** Intracellular accumulation of BaP in ZF-L cells exposed to BaP with or without fullerene
655 C_{60} (1.0mg/L). **C**: Milli Q water control. **D**: dimethyl sulfoxide (DMSO) control. **(a)** Accumulation
656 kinetics of BaP (1.00 µg/L) throughout 4 h of exposure; data are expressed as percentages of the
657 control group. **(b)** Fluorescence units from the readings in samples without cells after 4 h of
658 incubation to BaP (0.01, 0.10 or 1.00 µg/L). Same letters indicate the absence of statistically
659 significant ($p>0.05$) differences. N= 3 to 4 independent experiments.

660

661 **Figure 5.** Reactive oxygen species (ROS) concentration after 4 h of exposure to BaP (0.01, 0.10 or
662 1.00 µg/L) with or without fullerene C_{60} (1.0 mg/L). C: Milli Q water control. D: dimethyl sulfoxide
663 (DMSO) control. Data are expressed as relative fluorescence area adjusted to the number of viable

664 cells of each treatment. Same letters indicate the absence of statistically significant ($p>0.05$)
665 differences. N= 3 to 4 independent experiments.
666
667 **Figure 6.** Specific activity of glutathione-S-transferase (GST) in ZF-L cells exposed for 4 h to BaP
668 (0.01, 0.10 or 1.00 µg/L) with or without fullerene C_{60} (1.0 mg/L). **C**: Milli Q water control. **D**:
669 dimethyl sulfoxide (DMSO) control. Same letters indicate the absence of statistically significant
670 ($p>0.05$) differences. N= 3 to 8 independent experiments.
671
672 **Figure 7. (a)** Scheme of pi glutathione-S-transferase (GST) isoform, showing the binding site of
673 glutathione and the HEPES allosteric site where fullerene C_{60} showed the highest affinity. **(b)**
674 Amino acid residues close to fullerene C_{60}. The model shows the interaction with lysine residue
675 188.
676

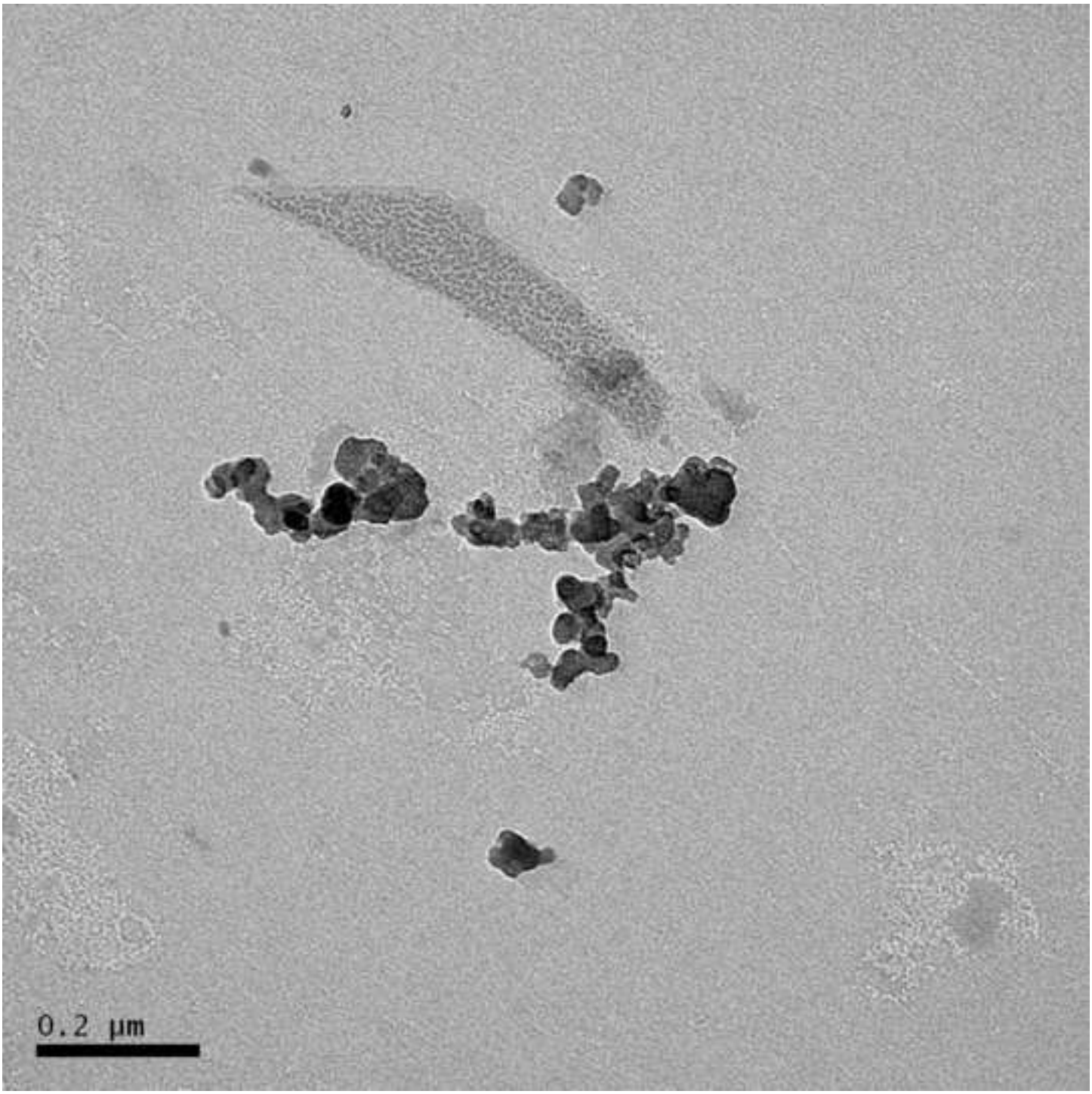

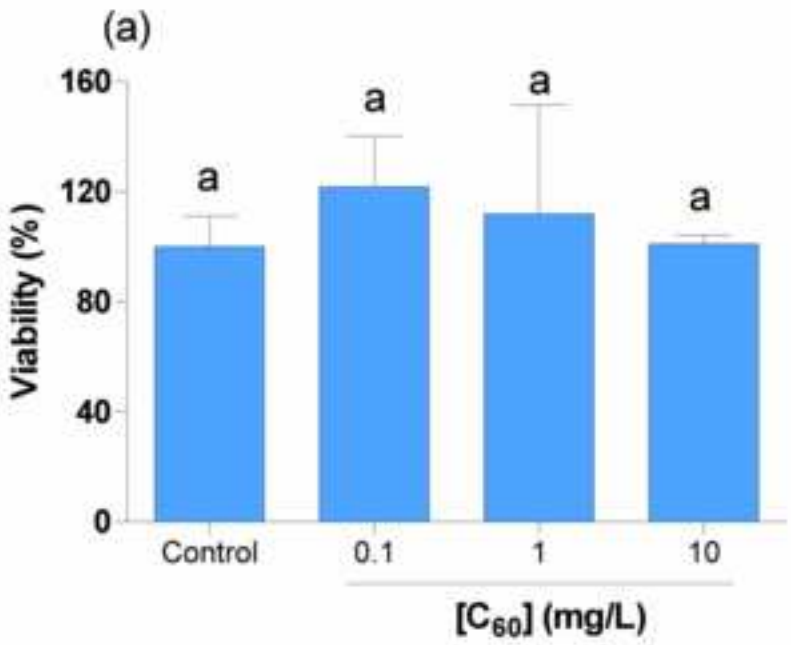

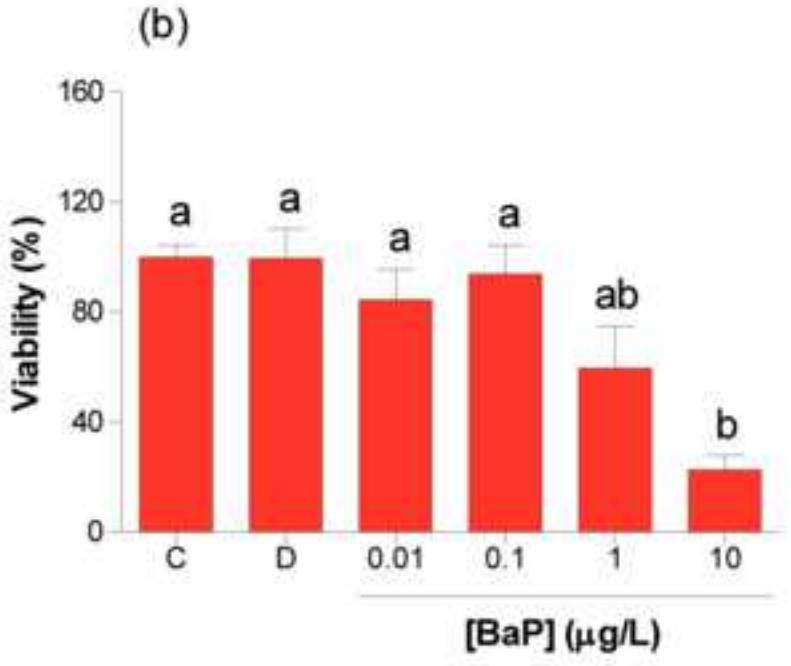

Figure 3

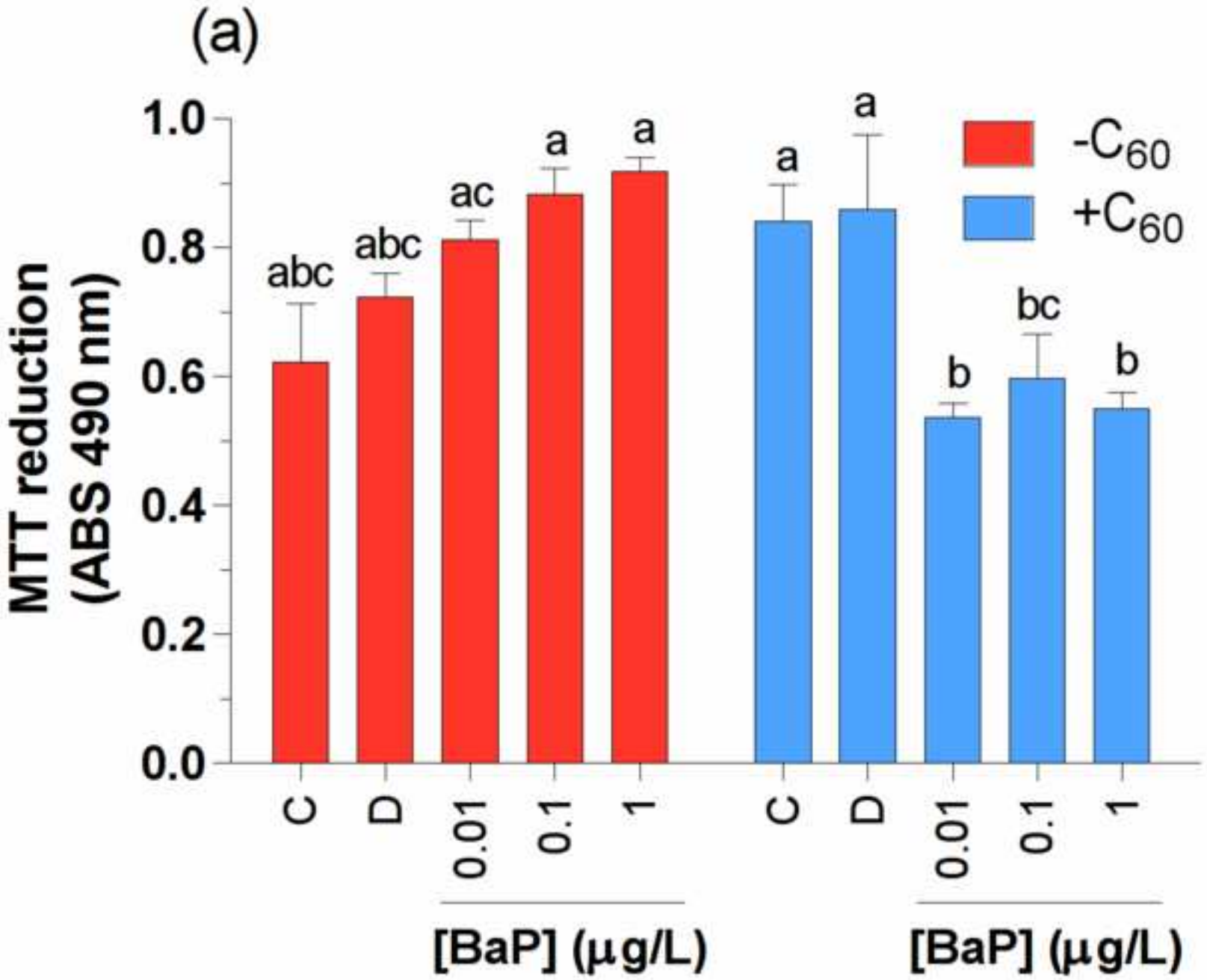
(a)
MTT reduction (ABS 490 nm)
1.0
0.8
0.6
0.4
0.2
0.0
abc
abc
ac
a
a
a
a
b
bc
b
-C60
+C60
C
D
0.01
0.1
1
[BaP] (µg/L)

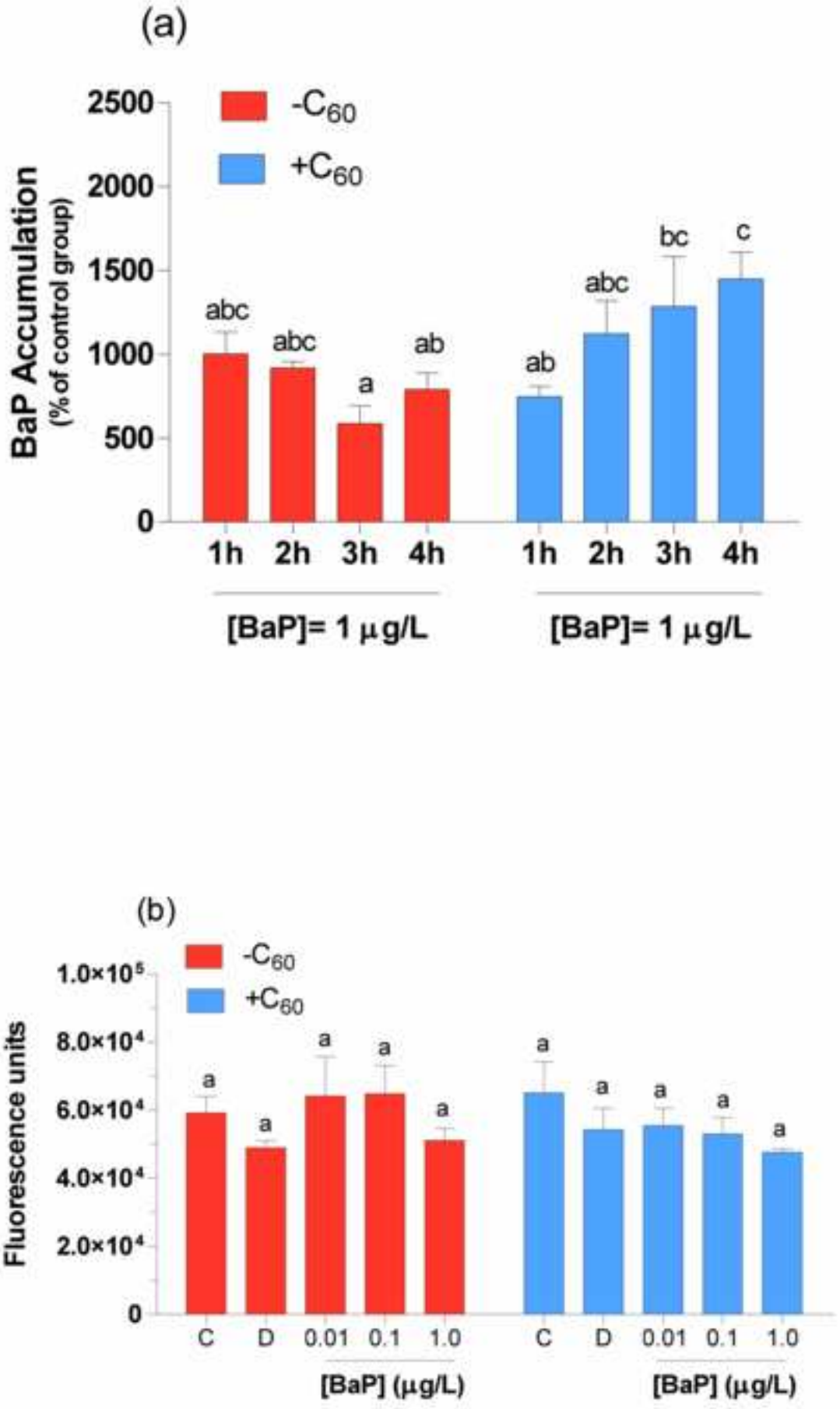

Figure 5

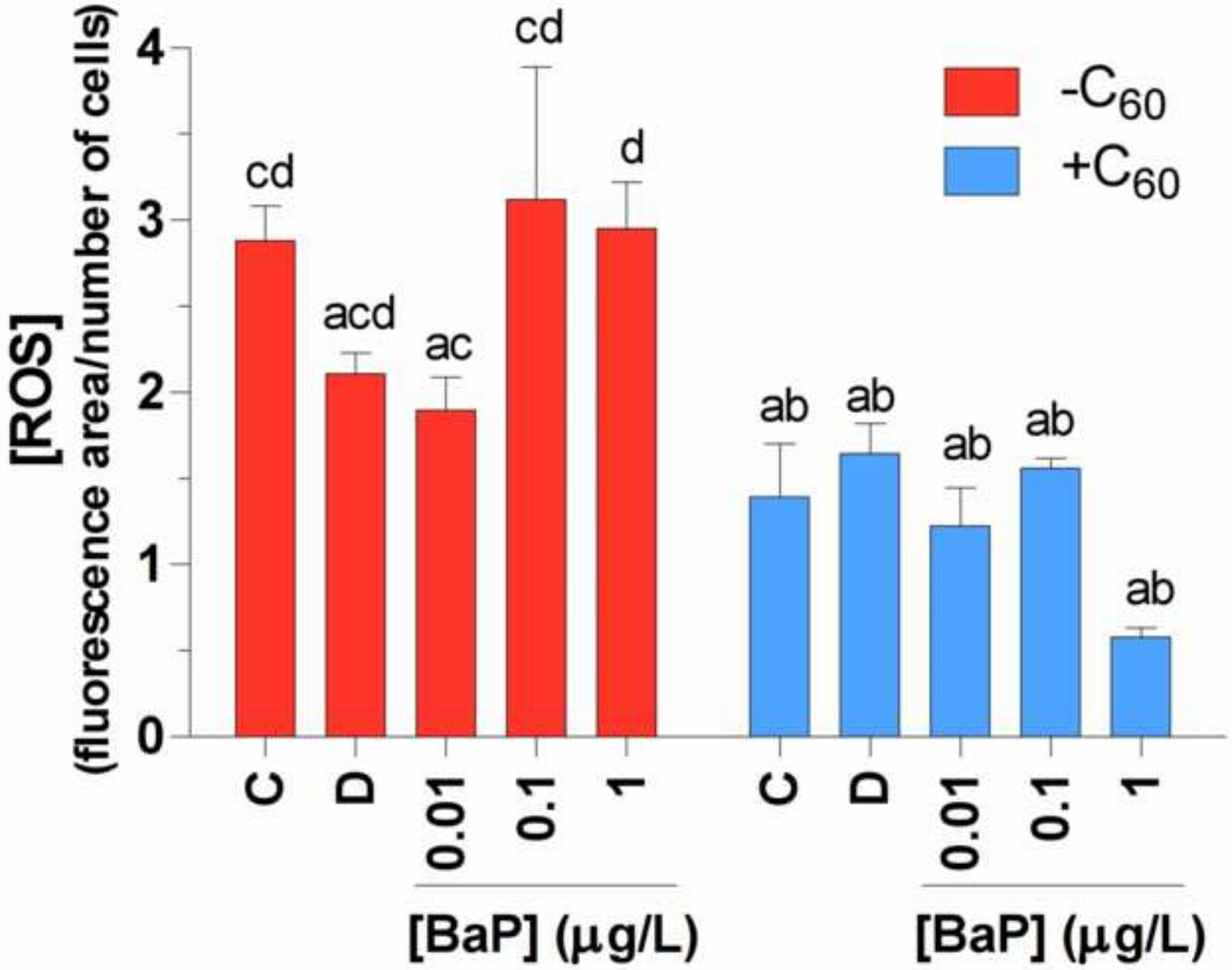
[ROS]
(fluorescence area/number of cells)
4
3
2
1
0
cd
acd
ac
cd
d
ab
ab
ab
ab
ab
-C60
+C60
C
D
0.01
0.1
1
[BaP] (µg/L)
[BaP] (µg/L)

Figure 6

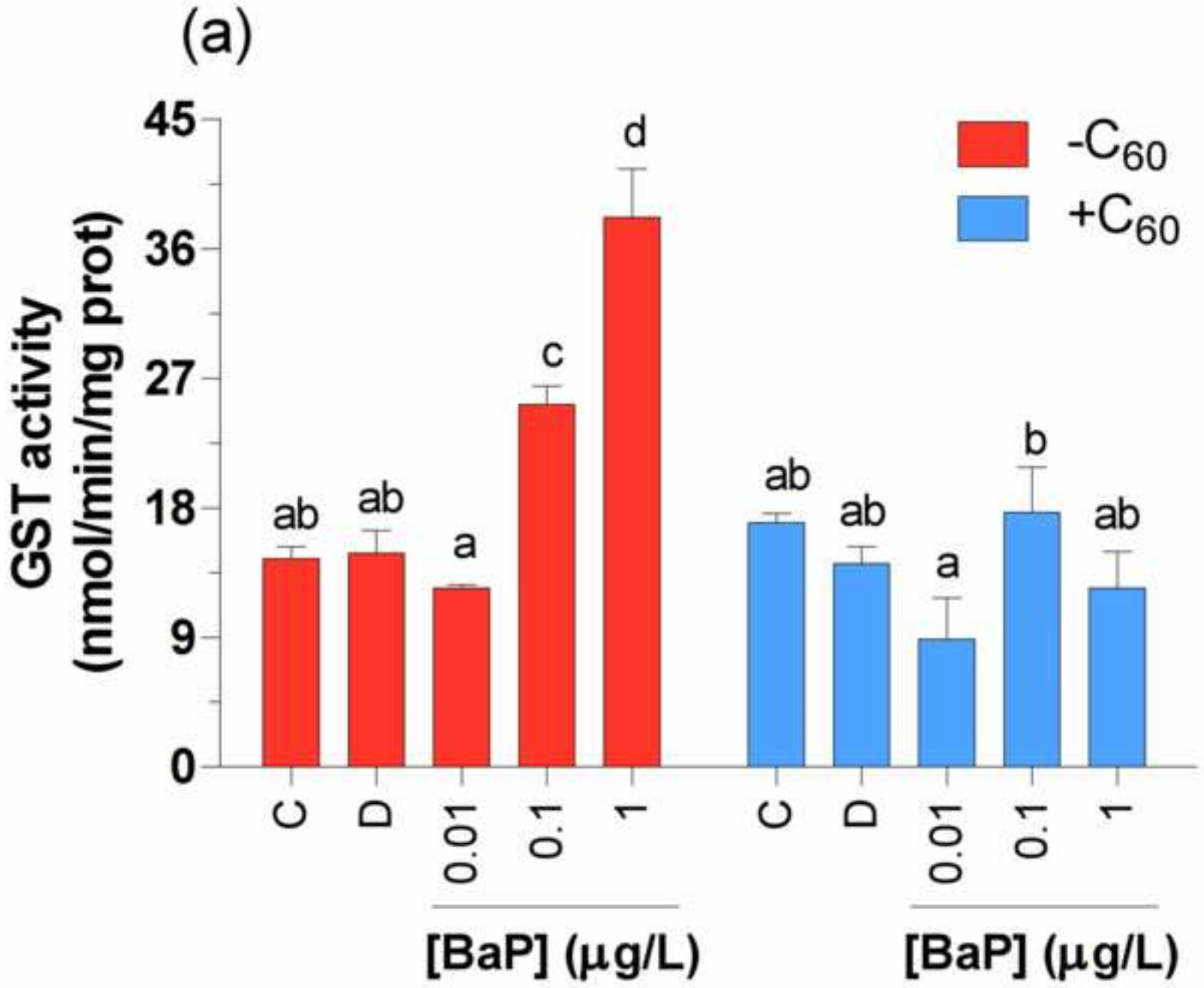
(a)
GST activity (nmol/min/mg prot)
45
36
27
18
9
0
-C60
+C60
ab
ab
a
c
d
ab
ab
a
b
ab
C
D
0.01
0.1
1
C
D
0.01
0.1
1
[BaP] (µg/L)
[BaP] (µg/L)

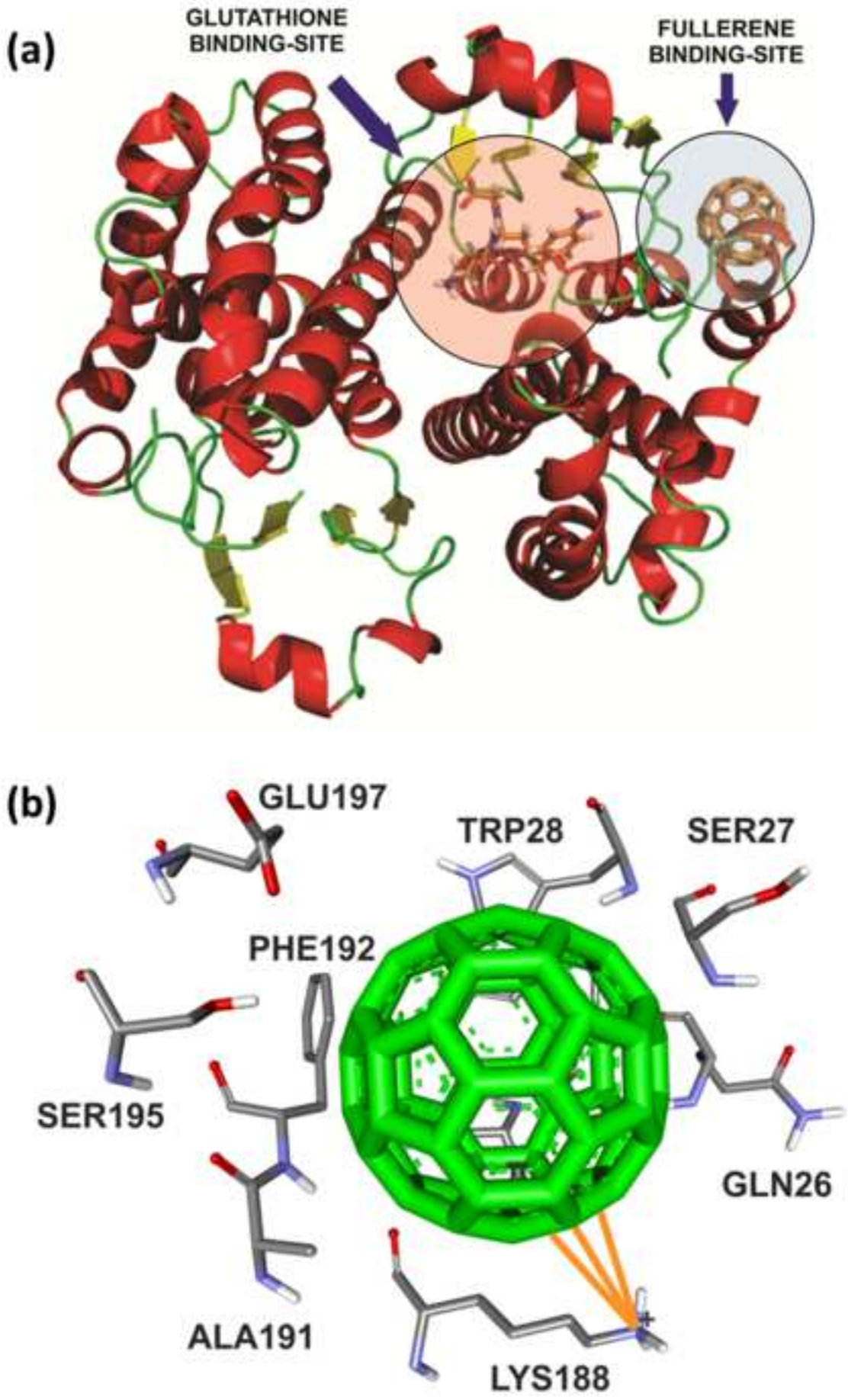

Highlights

– Fullerene C60 and PAH benzo[a]pyrene (BaP) synergistic effects were tested.
– C_{60} increased cellular intake of BaP.
– C_{60} decreased cell viability and phase II detoxificatory response triggered by BaP.
– *In silico*, C_{60} molecule can inhibit the enzyme glutathione-S-transferase.
– C_{60} can increase toxicity of PAHs possibly through delivery mechanisms.